Fellow, 1976–1978.
(3) C. Creutz and H. Taube, *J. Am. Chem. Soc.*, **91**, 3988 (1969).
(4) B. C. Bunker, R. S. Drago, D. N. Hendrickson, S. L. Kessel, and R. Richman, *J. Am. Chem. Soc.*, **100**, 3805 (1928).
(5) H. W. Richardson, J. R. Wasson, and W. E. Hatfield, *Inorg. Chem.*, **16**, 484 (1977).
(6) R. C. E. Belford, D. E. Fenton, and M. E. Truter, *J. Chem. Soc., Dalton Trans.*, 17 (1974).
(7) H. W. Richardson and W. E. Hatfield, *J. Am. Chem. Soc.*, **98**, 835 (1976).
(8) P. J. Hay, J. C. Thibeault, and R. Hoffmann, *J. Am. Chem. Soc.*, **97**, 4884 (1975).
(9) M. K. Child and G. C. Percy, *Spectrosc. Lett.*, **10**, 71 (1977).
(10) C. Su, J. W. Reed, and E. S. Gould, *Inorg. Chem.*, **12**, 337 (1973).
(11) R. A. Rowe and M. M. Jones, *Inorg. Synth.*, **5**, 114 (1957).
(12) R. C. E. Belford, D. E. Fenton, and M. R. Truter, *J. Chem. Soc., Dalton Trans.*, 2208 (1972).
(13) T. C. Kuechler, Ph.D. Thesis, University of Illinois, 1977, p 91.
(14) D. M. Duggan, E. K. Barefield, and D. N. Hendrickson, *Inorg. Chem.*, **12**, 985 (1973).
(15) B. N. Figgis and J. Lewis in "Modern Coordination Chemistry", J. Lewis and R. G. Wilkins, Ed., Interscience, New York, N.Y., 1960, p 403.
(16) J. P. Chandler, Program 66, Quantum Chemistry Program Exchange, Indiana University, Bloomington, Ind., 1973.
(17) E. J. Laskowski, T. R. Felthouse, and D. N. Hendrickson, *Inorg. Chem.*, **16**, 1077 (1977).
(18) J. A. Pople and D. L. Beveridge, "Approximate Molecular Orbital Theory", McGraw-Hill, New York, N.Y., 1970.
(19) See paragraph at end of paper regarding supplementary material.
(20) B. Bleaney and K. D. Bowers, *Proc. R. Soc. London, Ser. A*, **214**, 451 (1952).
(21) W. E. Hatfield in "Theory and Applications of Molecular Paramagnetism", E. A. Boudreaux and L. N. Mulay, Ed., Wiley, New York, N.Y., 1976, Chapter 7, p 349.
(22) A. P. Ginsbert, R. L. Martin, R. W. Brookes, and R. C. Sherwood, *Inorg. Chem.*, **11**, 2884 (1972).
(23) D. M. Duggan and D. N. Hendrickson, *Inorg. Chem.*, **13**, 1911 (1974).
(24) E. J. Laskowski, D. M. Duggan, and D. N. Hendrickson, *Inorg. Chem.*, **14**, 2449 (1975).
(25) T. R. Felthouse, E. N. Duesler, and D. N. Hendrickson, *J. Am. Chem. Soc.*, **100**, 618 (1978).
(26) P. C. Jain and E. C. Lingafelter, *J. Am. Chem. Soc.*, **89**, 724 (1967).
(27) H. Taube, "Bioinorganic Chemistry-II", *Adv. Chem. Ser.*, **No. 162** (1977).
(28) J. A. Merritt and K. K. Innes, *Spectrochim. Acta*, **16**, 945 (1960).
(29) T. R. Felthouse and D. N. Hendrickson, *Inorg. Chem.*, **17**, 2636 (1978).
(30) G. A. Senyukova, I. D. Mikheikin, and K. I. Zamarev, *Russ. J. Struct. Chem. (Engl. Transl.)*, 11, 18 (1970).
(31) R. Barbucci and M. J. M. Campell, *Inorg. Chim. Acta*, **15**, L15 (1975).
(32) R. Barbucci, A. Bencini, and D. Gatteschi, *Inorg. Chem.*, **16**, 2117 (1977).
(33) P. Ford, De F. P. Rudd, R. Gaunder, and H. Taube, *J. Am. Chem. Soc.*, **90**, 1187 (1968).
(34) R. S. Drago, T. C. Kuechler, and M. Kroeger, submitted for publication.
(35) M. Sekizaki, K. Yamasaki, and K. Hayashi, *Nippon Kagaku Zasshi*, **91**, 1191 (1970).
(36) P. W. Carreck, M. Goldstein, E. M. McPartlin, and W. D. Unsworth, *Chem. Commun.*, 1634 (1971).
(37) R. W. Matthews and R. A. Walton, *Inorg. Chem.*, **10**, 1433 (1971).
(38) M. Inoue and M. Kubo, *Coord. Chem. Rev.*, **21**, 1 (1976).

Preparations and Properties of Nitrosyl Complexes of Iron Tetramethylcyclam. X-ray Structures of $[Fe(C_{14}H_{32}N_4)NO](BF_4)_2$, a $S = \frac{3}{2}$–$\frac{1}{2}$ Spin-Equilibrium Complex, and $[Fe(C_{14}H_{32}N_4)(NO)(OH)](ClO_4)_2 \cdot CH_3CN$

Keith D. Hodges,[1a,b] R. G. Wollmann,[1b] S. L. Kessel,[1b] D. N. Hendrickson,*[1b,c] D. G. Van Derveer,[1a] and E. Kent Barefield*[1a]

Contribution from the School of Chemistry, Georgia Institute of Technology, Atlanta, Georgia 30332, and the School of Chemical Sciences, University of Illinois, Urbana, Illinois 61801. *Received July 13, 1978*

Abstract: Reactions of $[Fe(TMC)(NCCH_3)](BF_4)_2$ (TMC = 1,4,8,11-tetramethyl-1,4,8,11-tetraazacyclotetradecane) with $NO_{(g)}$ in CH_3NO_2 and $NOBF_4$ in CH_3CN yield green, paramagnetic $[Fe(TMC)NO](BF_4)_2$ and red, diamagnetic $[Fe(TMC)(NO)(OH)](BF_4)_2 \cdot CH_3CN$, respectively. The hydroxyl group in the latter complex apparently comes from water impurities in the CH_3CN. Physical and chemical properties of these complexes are reported. Of note is the temperature-dependent magnetic moment of $[Fe(TMC)NO](BF_4)_2$, which ranges from 3.62 μ_B at 286 K to 2.66 μ_B at 4.2 K. IR, EPR, and Mössbauer data support a $S = \frac{3}{2}$–$\frac{1}{2}$ spin equilibrium for the complex. Single-crystal, X-ray structures of $[Fe(TMC)NO](BF_4)_2$ and $[Fe(TMC)(NO)(OH)](ClO_4)_2 \cdot CH_3CN$ (obtained by metathesis of the BF_4^- salt) are also described. $[Fe(TMC)NO](BF_4)_2$ crystallizes in space group $P2_1/c$ with four molecules in a cell of dimensions $a = 8.658$ (5) Å, $b = 17.317$ (5) Å, $c = 15.132$ (8) Å; $\beta = 91.93$ (4)°, $\rho_{calcd} = 1.51$ g cm^{-3}, $\rho_{obsd} = 1.49$ (2) g cm^{-3}. Full-matrix least-squares refinement of 2777 reflections having $I > 3\sigma_I$ gave $R = 0.060$ and $R_w = 0.059$. The cation is five-coordinate with the nitrosyl group in the apical position of a distorted tetragonal pyramid; the Fe–N–O angle is 177.5 (5)° with Fe–NO and FeN–O interatomic distances of 1.737 (6) and 1.137 (6) Å, respectively. The electronic structure of this unusual nitrosyl complex is described by a modified $\{FeNO\}^7$ model. The hydroxy-nitrosyl complex crystallizes in space group $P\bar{1}$ with two molecules in a cell of dimensions $a = 10.823$ (4) Å, $b = 14.489$ (4) Å, $c = 14.489$ (4) Å; $\alpha = 134.61$ (2)°, $\beta = 108.97$ (2)°, $\gamma = 98.47$ (3)°, $\rho_{calcd} = 1.61$ g cm^{-3}, $\rho_{obsd} = 1.57$ (2) g cm^{-3}. Full-matrix, least-squares refinement of 3027 reflections having $I > 3\sigma_I$ gave $R = 0.067$ and $R_w = 0.064$. The cation consists of six-coordinate iron, axially coordinated by the NO and OH groups. As in the $[Fe(TMC)NO]^{2+}$ cation, the axially oriented *N*-methyl groups are all on the same side of the Fe–TMC moiety as the nitrosyl group. This is the first structurally characterized six-coordinate complex of TMC having this set of nitrogen configurations. The Fe–N–O angle is 178.3 (6)° with Fe–NO and Fe–OH interatomic distances of 1.621 (6) and 1.798 (3) Å, respectively. The iron atom is 0.156 Å out of the N_4 plane toward the nitrosyl ligand.

Introduction

Macrocyclic tetramine **I** (1,4,8,11-tetramethyl-1,4,8,11-tetraazacyclotetradecane, abbreviated TMC)[2a] binds metal ions in a stereospecific fashion such that the four *N*-methyl substituents lie on the same side of the metal–nitrogen plane as shown by **II**.[2b] This extreme differentiation of the two sides

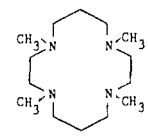

I

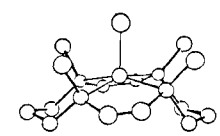

II

0002-7863/79/1501-0906$01.00/0

of the four-coordinate complex ion results in a marked propensity for formation of five-coordinate complexes by addition of a fifth donor as shown by early studies on Co, Ni, Cu, and Zn complexes.[2,3] The X-ray structure of $[Ni(TMC)N_3]ClO_4$ shows that the azide ion is bonded to the nickel ion on the *N*-methyl side of the complex.[2b] The same structure is believed to apply to all five-coordinate complexes of the ligand. The only complex prepared in our earlier studies that appears to be a six-coordinate species is $[Ni(TMC)(NCS)_2]$.[2a] Its structure is unknown.

More recently the unique stereochemical influence of I was utilized in the preparation of five-coordinate iron(II) complexes for a detailed study of zero-field splitting of a d^6 metal ion in this geometry.[4] In an extension of our work with the iron–TMC system we have investigated reactions of the Fe–TMC complex with nitrosyl ligands, the subject of this report. We began this study with the expectation that we might be able to prepare $[Fe(TMC)NO]^{2+/3+}$ ($\{FeNO\}^7$ and $\{FeNO\}^6$ by the nomenclature introduced by Feltham and Enemark[5]) by reactions of $[Fe(TMC)NCCH_3]^{2+}$ with NO and NO^+. In spite of the voluminous literature on transition metal nitrosyls, only a few examples of five-coordinate $\{MNO\}^7$ (see ref 15 and 19 for these examples) and only a single example of five-coordinate $\{MNO\}^6$ are known.[5] Thus the preparation of examples of such species would provide additional tests of current theories of bonding in metal nitrosyls and perhaps allow extensions of these ideas. Our interest was considerably heightened in the early stages of this work by the discovery that the nitrosyl complex $[Fe(TMC)NO)](BF_4)_2$ apparently has a $S = 3/2$ spin state at room temperature and a temperature-dependent magnetic moment. As far as we know, [Fe(salen)NO] and some of its ring-substituted derivatives are the only five-coordinate $\{FeNO\}^7$ species reported to have anything other than an $S = 1/2$ spin state.[6] These compounds also show reduced moments at low temperature.

This paper reports the preparation, X-ray structure, physical methods characterization, and reactivity studies of $[Fe(TMC)NO](BF_4)_2$. Also included are the synthesis and characterization of $[Fe(TMC)(NO)(OH)]Y_2 \cdot CH_3CN$ ($Y = BF_4^-$ or ClO_4^-) and the X-ray structure of the perchlorate salt.

Experimental Section

Materials. All operations were performed under an atmosphere of N_2 unless otherwise specified. All solvents were dried by appropriate methods and degassed prior to use. Nitrosonium tetrafluoroborate (Ozark-Mahoning) was sublimed (200°C, 10^{-5} mmHg) before use. Nitric oxide was passed through a trap of KOH pellets before use. $[Fe(TMC)NCCH_3](BF_4)_2$ was prepared by the published procedure.[4]

$[Fe(TMC)NO](BF_4)_2$. Isomer AB. Approximately 1 g of $[Fe(TMC)NCCH_3](BF_4)_2$ was ground to a fine powder in an agate mortar. The powdered material was transferred to a vial which was placed in a 250-mL pressure bottle.[7] The bottle was evacuated (5×10^{-2} mmHg) and subsequently charged with 50 psig NO. Although the pale blue powder turned deep green almost immediately, the reaction was not complete for several days. After complete reaction no C≡N stretching absorption was detectable in the product. Anal. Calcd for $FeC_{14}H_{32}N_5OBF_4$: C, 32.59; H, 6.25; N, 13.57; Fe, 10.82. Found: C, 32.84; H, 6.05; N, 13.63; Fe, 10.87.

Isomer A. $[Fe(TMC)NCCH_3](BF_4)_2$ (0.5 g) was dissolved in 10 mL of CH_3NO_2 contained in a flask fitted with a serum cap. Nitric oxide was bubbled through the well-stirred pale pink solution for 10 min, during which time a deep green color developed. Slow addition of 20 mL of ice-cold Et_2O saturated with NO caused a deep green, microcrystalline solid to form. The solid was collected in a nitrogen atmosphere, washed twice with ether, and dried briefly in vacuo, yield 0.38 g, 78%. Anal. Found: C, 32.51; H, 6.26; N, 13.46; Fe, 10.85. Crystallographic quality crystals were grown by slow diffusion of ether into a nitromethane solution of isomer A, with the entire system kept under an NO atmosphere.

$[Fe(TMC)(NO)(OH)](BF_4)_2 \cdot CH_3CN$. This complex could be prepared in a reproducible manner by treatment of an acetonitrile solution of $[Fe(TMC)NCCH_3](BF_4)_2$ (ca. 500 mg in 20 mL) with an excess of $NOBF_4$ followed by exposure of the resultant green solution to air for about 0.5 h. During this time the green color gradually changed to red. Filtration of the red solution, followed by addition of CH_2Cl_2 to the cloud point and cooling in a freezer for several hours, gave red crystals of the product which were collected, washed with ether, and dried in vacuo. Yields were ca. 50%. If necessary the material could be recrystallized from a minimum amount of boiling CH_3CN by cooling. Exposure of either the solid complex or its solutions to bright light was avoided, as it is photochemically sensitive. Anal. Calcd for $FeC_{16}H_{36}N_6O_2B_2F_8$: C, 33.48; H, 6.32; N, 14.64, Fe, 9.73. Found: C, 33.46; H, 6.07; N, 14.47; Fe, 9.75. Alternatively, bubbling NO into solutions of $[Fe(TMC)NCCH_3](BF_4)_2$ in CH_3CN (0.5 g in 15 mL) for 15 min and exposure of the resultant deep green solutions to air for 0.5 h resulted in the formation of the same red solutions. Isolation of an identical complex was accomplished as described above. Yields from this method were ca. 40%.

$[Fe(TMC)(NO)(OH)](ClO_4)_2 \cdot CH_3CN$. *Caution!* This compound constitutes an explosion hazard and should be handled in very small quantities with appropriate precautions. Dissolution of $[Fe(TMC)(NO)(OH)](BF_4)_2 \cdot CH_3CN$ in slightly more than the minimum amount of CH_3CN and addition of a saturated solution of $NaClO_4$ in CH_3CN caused the precipitation of a red solid. The powder was collected, dissolved in the minimum amount of boiling CH_3CN, filtered, and cooled overnight in a freezer. The red crystals which deposited were collected, washed with ether, and dried briefly in vacuo. The yield was nearly quantitative. Anal. Calcd for $FeC_{16}H_{36}N_6Cl_2O_{10}$: C, 32.07; H, 6.06; N, 14.02; Fe, 9.32; Cl, 11.83; O, 26.69. Found: C, 32.12; H, 5.78; N, 14.01; Fe, 9.39; Cl, 11.56; O, 25.95. Crystals for structure analysis were obtained by slow evaporation of an acetonitrile solution *in the dark*.

$\{[Fe(TMC)OH]_2TMC \cdot H_2\}(ClO_4)_6 \cdot xH_2O$. An acetonitrile solution of $[Fe(TMC)(NO)(OH)](ClO_4)_2 \cdot CH_3CN$ was allowed to stand exposed to air and light for several days. The red solution turned yellow over several days and an off-white solid crystallized After removal of the white solid (shown to be a perchlorate salt of $TMC \cdot H_x^{x+}$ by infrared spectroscopy) the acetonitrile was evaporated to yield a yellow solid. This solid was recrystallized from dilute aqueous $HClO_4$ by slow evaporation to yield bright yellow crystals, which were collected, washed with THF, and dried in vacuo overnight. The use of the BF_4^- salt as starting material does not alter the sequence of events except that the recrystallization from water must be conducted in the dilute $HClO_4$ to obtain the highly crystalline perchlorate salt. Yields in several attempts were consistently less than 50%. Anal. Calcd for $Fe_2C_{42}H_{100}N_{12}Cl_6O_{26}$: Fe, 7.38; C, 33.30; H, 6.66; N, 11.10; Cl, 14.06. Calcd for the dihydrate: Fe, 7.21; C, 32.53; H, 6.50; N, 10.84; Cl, 13.73. Found: Fe, 7.07, 7.45; C, 32.56, 32.50; H, 6.42, 6.46; N, 10.88, 10.83; Cl, 13.57. pH titration of 31.3 mg of this complex required 0.420 mL of 0.098 M NaOH, which establishes an equivalent weight of 760 for the complex. Λ_M was 410 Ω^{-1} cm^2 mol^{-1} for a 6.9×10^{-4} M nitromethane solution.

Reaction of $[Fe(TMC)NCCH_3](BF_4)_2$ with $NOBF_4$ in CH_3CN or CH_2Cl_2. Addition of the acetonitrile complex to CH_3CN solutions of $NOBF_4$ resulted in immediate formation of deep green solutions. Even when highly purified reagents were used, the lifetime of the green species was highly variable (minutes to hours) and attempts to crystallize the complex were totally unsuccessful. In one experiment, 0.5 g of the acetonitrile complex was added to 20 mL of dry CH_2Cl_2 containing suspended $NOBF_4$ and the mixture stirred vigorously. After 24 h, the resulting green solid was collected, washed with CH_2Cl_2 and ether, and dried in vacuo. Anal. Calcd for $FeC_{14}H_{32}N_5OBF_4$: Fe, 9.27; C, 27.89; H, 5.35; N, 11.62. Found: Fe, 8.40; C, 27.98; H, 5.64; N, 11.35. We were not successful in obtaining satisfactory analytical data for subsequent preparations.

Physical Measurements. Variable-temperature magnetic susceptibility measurements were made with a PAR Model 150A vibrating sample magnetometer. Samples of $CuSO_4 \cdot 5H_2O$ were used as a standard in conjunction with a calibrated GaAs diode. Variable-temperature IR spectra were obtained on 13-mm KBr pellets of the various compounds employing a CTI Spectrim closed-cycle refrigerator.

Iron-57 Mössbauer data were collected at various temperatures using spectrometers that have been previously described.[4] Isomer shifts are referenced to iron metal.

Crystallographic Data Collection. $[Fe(TMC)NO](BF_4)_2$. A crystal exhibiting six faces with approximate dimensions 0.3 × 0.4 × 0.4 mm was mounted on a glass fiber and coated with epoxy cement such that a long crystal dimension was approximately parallel to the fiber direction.

Unit cell parameters and the orientation matrix were determined on a Syntex $P2_1$ four-circle diffractometer equipped with a graphite monochromator (Bragg 2θ angle = 12.2°) using Mo Kα radiation at a takeoff angle of 6.5°. Fifteen reflections whose 2θ values ranged from 5.84 to 17.19° were machine centered and used in least-squares refinement of the lattice parameters and orientation matrix. Unit cell parameters are a = 8.658 (5) Å, b = 17.317 (5) Å, c = 15.132 (8) Å, β = 91.93 (4)°, and V = 2267 (2) Å^3. The calculated density of 1.51 g cm^{-3} for four formula weight units per cell agrees with the experimental density of 1.49 (2) g cm^{-3} measured by the flotation method in hexane and CCl_4. ω scans of several low 2θ angle reflections gave peak widths at half-weight of less than 0.28°, indicating a satisfactory mosaic spread for the crystal.

Axial photographs indicated that the crystal belonged to the monoclinic system. Intensity data for zero and upper levels were collected at a rapid scan rate and the intensities examined carefully for systematic absences. The absence of $h0l$, $l = 2n + 1$; $0k0$, $k = 2n + 1$, is consistent only with space group $P2_1/c$ (no. 14).[8]

Intensity data were collected using θ-2θ scans with X-ray source and monochromator settings identical with those used for the determination of the unit cell parameters. A variable scan rate of 3.9–29.3° min^{-1} was used and a scan width of 2.3° was sufficient to collect all of the peak intensity. Stationary background counts were made at the beginning (bgd1) and at the end (bgd2) with a total background to scan time ratio, TR, of 1.0. No significant fluctuations were observed in the intensities of the three standard reflections (0, 0, 8), (0, 10, 0), (4, 0, 0) monitored every 97 reflections. Intensities were calculated from the total scan count (CT) and background counts by the relationship

$$I = CT - (TR)(bgd1 + bgd2)$$

The intensities were assigned standard deviations according to the formula

$$\sigma(I) = [CT + (TR)^2(bgd1 + bgd2)]^{1/2}$$

From a total of 4346 reflections collected in a complete quadrant ($\pm h$, $+k$, $+l$) of data out to 2θ = 50°, 2777 were accepted as statistically above background on the basis that I was greater than $3\sigma_I$. Lorentz and polarization corrections were made but no correction was made for absorption (μ = 7.6 cm^{-1}).

$[Fe(TMC)(NO)(OH)](ClO_4)_2 \cdot CH_3CN$. A red crystal with approximate dimensions 0.25 × 0.3 × 0.5 mm was mounted on a glass fiber using epoxy cement such that the longest crystal dimension (1,0,0) was approximately parallel to the fiber axis.

Unit cell parameters and the orientation matrix were determined on a Syntex $P2_1$ four-circle diffractometer as described above. The 15 reflections used for centering and least-squares refinement of the lattice parameters had 2θ values ranging from 8.79 to 19.59°.

Unit cell parameters are a = 10.823 (4) Å, b = 14.489 (4) Å, c = 14.489 (4) Å, α = 134.61 (2)°, β = 108.97 (2)°, γ = 98.47 (3)°, and V = 1270 (1) Å^3. The calculated density of 1.61 g cm^{-3} for two formula weight units per unit cell agrees well with the experimental density of 1.57 (2) g cm^{-3} measured by the flotation method using $CHBr_3$ and CCl_4. ω scans of several low 2θ reflections gave peak widths at half-height of less than 0.28° indicating a satisfactory mosaic spread for the crystal.

Axial photographs indicated that the crystal belonged to the triclinic system. Intensity data for zero and upper levels were collected at a rapid scan and the intensities examined carefully for systematic absences. No systematic absences were found, consistent only with space group $P1$ or $P\bar{1}$ (no. 1 or 2).[8] $P\bar{1}$ was assumed and successful refinement of the structure in this space group confirms this choice.

Intensity data were collected using θ-2θ scans with X-ray source and monochromator settings identical with those used for the determination of the unit cell parameters. A variable scan rate of from 3.92 to 29.3° min^{-1} was used and a scan width of 2.2° was sufficient to collect all of the peak intensity. Stationary background counts were measured at the beginning (bgd1) and at the end (bgd2) of each scan with a total background to scan time ratio, TR, of 1.0. No significant fluctuations were observed in the intensities of three standard reflections (0,0,4; 0,6,1; 7,0,0) monitored every 97 reflections. Intensities and standard deviations were calculated as above. From a total of 4762 reflections collected in a complete hemisphere ($\pm h$, $\pm k$, $+l$) of data out to 2θ = 50.0°, 3027 were accepted as statistically above background on the basis that I was greater than $3\sigma_I$. Lorentz and polarization corrections were made, but no corrections for absorption were made (μ = 9.1 cm^{-1}).

$[Fe(TMC)NCCH_3](BF_4)_2$. A nearly spherical crystal ~0.3 mm in diameter was lodged in a capillary with Dow-Corning Silicone grease. Unit cell parameters and the orientation matrix were determined as described above. Unit cell parameters are a = 9.622 Å, b = 9.622 Å, c = 13.511 Å. The calculated density of 1.398 g cm^{-3} for two formula weights per unit cell agrees with the experimental density of 1.40 (2) g cm^{-3} measured by flotation in hexane/CCl_4. Axial photographs indicated that the crystal belonged to the tetragonal system. Intensity data for zero and upper levels showed $hk0$, $h + k = 2n + 1$, to be systematically absent. This absence is consistent with space group $P4/n$ or $P4/nmm$ (no. 85 or 129).[8] Both of these space groups require that the iron atom occupy a position on a fourfold rotational axis. Since the tetramine ligand can only have C_{2v} symmetry at best, the structure must be extensively disordered. Nonetheless an attempt was made to refine the structure in the $P4/n$ space group. The position of the iron atom was determined from a Patterson synthesis and refined by least-squares methods. The resulting electron density map was used to locate a nitrogen and two carbon atoms lying on the fourfold axis. The structure determination was abandoned after two further cycles of least-squares refinement of the positions of the iron and these three atoms since further atoms could not be located.

Solution and Refinement of Structures. All computations were carried out on a CDC Cyber 70/74 computer using standard programs. For structure factor calculations the scattering factors for all atoms except hydrogen were taken from Cromer and Waber's tabulation;[10] Stewart's hydrogen atom scattering factors[11] were used. The scattering factors for iron and chlorine were corrected for the real and imaginary anomalous dispersion components, using the dispersion factors given by Cromer.[12] The agreement factors are defined in the usual way as

$$R = \sum ||F_o| - |F_c|| / \sum |F_o|$$

and

$$R_w = [\sum w(|F_o| - |F_c|)^2 / \sum w(|F_o|)^2]^{1/2}$$

In all least-squares refinements the quantity minimized was $w(|F_o| - |F_c|)^2$. A weighting scheme based on counting statistics ($w = 4I/\sigma^2(I)^2$) was employed for calculating R_w and in least-squares refinement.

$[Fe(TMC)NO](BF_4)_2$. The position of the iron atom was deduced from a three-dimensional Patterson synthesis and refined by the least-squares method; the resulting electron density map was used to locate the position of two of the tertiary amine nitrogen atoms. Two cycles of least-squares refinement of these atoms gave R = 0.43. After location of the nitrosyl nitrogen and an additional tertiary amine nitrogen atom and refinement of these atoms, R = 0.4. Location of all nonhydrogen atoms of the cation and refinement gave R = 0.33. When the atoms of the two tetrafluoroborate anions were included in the refinement R dropped to 0.12. Anisotropic refinement of the iron atom, both nitrosyl group atoms, and the ten atoms of the BF_4^- groups gave R = 0.09. One or more of the hydrogen atoms attached to each carbon atom, except the CN(2) methyl, was subsequently located; the remaining hydrogen atom positions were calculated. All 29 of these atoms were included in the refinement in fixed positions with fixed isotropic thermal parameters of 5.0 to give R = 0.08. Two of the remaining hydrogen atoms were then located and the position of the last one was calculated. These were included, also in fixed positions, and all remaining nonhydrogen atoms refined anisotropically to give R = 0.060 and R_w = 0.059. After the final cycle of refinement the largest shift was 0.09 δ for the x coordinate of F(6). The largest peak in the final electron density map (1.25 e/Å^3) was in the vicinity of F(6).

Final positional and thermal parameters are listed in Tables I and II; a table of calculated and observed structure amplitudes may be obtained. (See paragraph at end of paper regarding supplementary material.) Selected interatomic distances, angles, and least-squares planes are tabulated in Table III.

$[Fe(TMC)(NO)(OH)](ClO_4)_2 \cdot CH_3CN$. The positions of the iron atom and one chlorine atom were determined from a three-dimensional

Table I. Final Positional and Anisotropic Thermal Parameters[a] (with esd's) for Nonhydrogen Atoms of $[Fe(TMC)(NO)](BF_4)_2$

atom	X	Y	Z	β_{11}	β_{22}	β_{33}	β_{12}	β_{13}	β_{23}
Fe	0.23964 (9)	0.10803 (4)	0.25247 (6)	0.0104 (1)	0.00264 (2)	0.00334 (3)	0.00064 (5)	0.00037 (4)	0.00015 (3)
N1	0.3870 (6)	0.1755 (3)	0.2658 (3)	0.0132 (7)	0.0043 (2)	0.0050 (3)	−0.0002 (4)	−0.0001 (3)	0.0004 (2)
O	0.4835 (6)	0.2200 (3)	0.2713 (4)	0.0224 (9)	0.0076 (3)	0.0082 (3)	−0.0064 (5)	−0.0012 (4)	0.0008 (2)
N2	0.1398 (5)	0.1254 (2)	0.3815 (3)	0.0152 (7)	0.0037 (2)	0.0040 (2)	0.0016 (3)	0.0008 (3)	0.0000 (2)
N3	0.3189 (6)	0.0012 (3)	0.3100 (3)	0.0184 (8)	0.0035 (2)	0.0042 (2)	0.0026 (3)	−0.0009 (3)	0.0004 (2)
N4	0.2935 (5)	0.0711 (3)	0.1202 (3)	0.0146 (7)	0.0038 (2)	0.0046 (2)	0.0016 (3)	0.0020 (3)	−0.0004 (2)
N5	0.0513 (5)	0.1676 (2)	0.1843 (3)	0.0131 (7)	0.0028 (2)	0.0041 (2)	0.0008 (3)	−0.0009 (3)	−0.0004 (2)
CN2	0.1868 (8)	0.2007 (4)	0.4231 (4)	0.020 (1)	0.0060 (3)	0.0048 (3)	0.0002 (5)	0.0003 (5)	−0.0015 (3)
CN3	0.4878 (8)	0.0018 (4)	0.3296 (5)	0.020 (1)	0.0043 (3)	0.0094 (5)	0.0033(5)	−0.0048 (6)	−0.0010 (3)
CN4	0.4579 (8)	0.0832 (4)	0.0970 (5)	0.021 (1)	0.0050 (3)	0.0077 (4)	0.0003 (5)	0.0064 (6)	−0.0000 (3)
CN5	0.0871 (7)	0.2518 (3)	0.1798 (4)	0.019 (1)	0.0034 (2)	0.0058 (3)	0.0009 (4)	−0.0005 (5)	0.0009 (2)
C1	0.211 (1)	0.0650 (5)	0.4384 (5)	0.030 (2)	0.0067 (4)	0.0044 (4)	0.0053 (7)	0.0029 (6)	0.0013 (3)
C2	0.232 (1)	−0.0055 (5)	0.3947 (5)	0.041 (2)	0.0047 (3)	0.0045 (4)	0.0040 (6)	0.0021 (7)	0.0018 (3)
C3	0.2817 (7)	−0.0693 (3)	0.2558 (5)	0.020 (1)	0.0033 (2)	0.0067 (4)	0.0020 (4)	0.0005 (5)	−0.0000 (3)
C4	0.3340 (7)	−0.0688 (3)	0.1630 (4)	0.019 (1)	0.0031 (2)	0.0066 (4)	0.0005 (4)	0.0013 (5)	−0.0015 (2)
C5	0.2523 (7)	−0.0111 (4)	0.1031 (4)	0.0148 (9)	0.0043 (3)	0.0052 (3)	0.0003 (4)	0.0008 (4)	−0.0007 (2)
C6	0.2013 (9)	0.1242 (4)	0.0612 (4)	0.028 (1)	0.0046 (3)	0.0038 (3)	0.0037 (5)	0.0013 (5)	0.0002 (2)
C7	0.0435 (8)	0.1346 (3)	0.0934 (4)	0.023 (1)	0.0040 (2)	0.0039 (3)	0.0026 (4)	−0.0032 (5)	−0.0003 (2)
C8	−0.1057 (7)	0.1576 (4)	0.2232 (4)	0.0137 (9)	0.0045 (3)	0.0064 (4)	0.0006 (4)	−0.0011 (5)	−0.0003 (2)
C9	−0.1138 (7)	0.1762 (4)	0.3203 (4)	0.0115 (8)	0.0057 (3)	0.0063 (4)	0.0024 (4)	0.0021 (4)	−0.0003 (3)
C10	−0.0316 (7)	0.1194 (4)	0.3806 (4)	0.018 (1)	0.0046 (3)	0.0048 (3)	−0.0005 (5)	0.0031 (4)	−0.0005 (2)
B1	−0.3830 (9)	0.2862 (4)	0.0191 (5)	0.021 (1)	0.0040 (3)	0.0047 (4)	−0.0001 (5)	0.0005 (6)	0.0001 (3)
F1	−0.4076 (5)	0.3503 (2)	−0.0322 (3)	0.0242 (7)	0.0064 (2)	0.0091 (3)	0.0012 (3)	−0.0008 (4)	0.0030 (2)
F2	−0.4853 (8)	0.2835 (3)	0.0835 (4)	0.050 (1)	0.0093 (3)	0.0093 (3)	−0.0021 (5)	0.0109 (6)	0.0004 (2)
F3	−0.2382 (7)	0.2963 (4)	0.0553 (5)	0.029 (1)	0.0119 (4)	0.0154 (5)	0.0013 (5)	−0.0090 (6)	0.0041 (4)
F4	−0.394 (1)	0.2244 (3)	−0.0296 (4)	0.093 (3)	0.0058 (2)	0.0112 (4)	−0.0067 (7)	0.0111 (8)	−0.0037 (3)
B2	0.169 (1)	0.4241 (5)	0.3075 (7)	0.019 (1)	0.0042 (3)	0.0093 (6)	−0.0013 (6)	0.0003 (8)	−0.0007 (4)
F5	0.0601 (4)	0.3807 (2)	0.3463 (3)	0.0187 (6)	0.0045 (1)	0.0087 (2)	−0.0010 (3)	0.0008 (3)	0.0008 (2)
F6	0.1249 (9)	0.4486 (4)	0.2306 (4)	0.063 (2)	0.0145 (4)	0.0129 (4)	−0.0209 (8)	−0.0185 (8)	0.0094 (4)
F7	0.2290 (6)	0.4803 (2)	0.3614 (3)	0.034 (1)	0.0045 (2)	0.0113 (3)	−0.0037 (3)	−0.0056 (5)	0.0001 (2)
F8	0.2951 (6)	0.3745 (3)	0.2992 (6)	0.0226 (8)	0.0084 (3)	0.0224 (7)	0.0001 (4)	0.0045 (6)	−0.0015 (3)

[a] The form of the expression defining the thermal ellipsoids is $\exp[-\beta_{11}h^2 - \beta_{22}k^2 - \beta_{33}l^2 - 2\beta_{12}hk - 2\beta_{13}hl - 2\beta_{23}kl]$.

Patterson synthesis. Two cycles of least-squares refinement of their positional and thermal parameters gave $R = 0.43$. All remaining nonhydrogen atoms were located from subsequent electron-density maps. Isotropic refinement of nonhydrogen atoms gave $R = 0.13$. Methylene proton positions were then calculated and positions for the methyl protons were determined from a combination of electron density map peaks and calculations. The perchlorate anion containing Cl2 was disordered and was refined with eight oxygen positions, each having a multiplier of 0.5. Final values of $R = 0.067$ and $R_w = 0.064$ were obtained by varying the positional parameters of all nonhydrogen atoms, isotropic thermal parameters for the disordered perchlorate oxygens, and anisotropic thermal parameters for the remaining nonhydrogen atoms. Hydrogen atom positions were not varied and their isotropic thermal parameters were fixed at 5.0. The largest shift in the final cycle of refinement was 0.1 δ. The highest residual electron density was in the vicinity of the perchlorate anions.

Final positional and thermal parameters are listed in Tables IV and V; a table of calculated and observed structure amplitudes may be obtained. (See paragraph at end of paper regarding supplementary material.) Selected interatomic distances, angles, and least-squares planes are tabulated in Table VI.

Results

Preparation and Characterization of Nitrosyl Complexes. Preparative aspects of the research are summarized in Scheme I. Compounds not isolated but for which some evidence was obtained are underlined. Evidence pertinent to the characterization of individual compounds is presented in the following sections.

$[Fe(TMC)NO](BF_4)_2$. Compounds of this stoichiometry can be prepared by two methods but the products have different physical properties. Good yields of a dark green, crystalline complex were obtained from the reaction of $[Fe(TMC)NCCH_3](BF_4)_2$ with $NO_{(g)}$ in CH_3NO_2. The infrared spectrum of this product (hereafter referred to as isomer A) exhibits a single NO stretching absorption at 1840 cm^{-1} both in the solid state (Nujol mull or KBr pellet) and solution

Table II. Final Positional Parameters (with esd's) for Hydrogen Atoms of $[Fe(TMC)(NO)](BF_4)_2$[a]

atom	X	Y	Z
HC1	0.156	0.061	0.492
HC1	0.316	0.084	0.457
HC2	0.125	−0.027	0.379
HC2	0.277	−0.045	0.432
HC3	0.172	−0.078	0.254
HC3	0.329	−0.114	0.285
HC4	0.321	−0.119	0.138
HC4	0.442	−0.056	0.165
HC5	0.145	−0.017	0.110
HC5	0.277	−0.023	0.044
HC6	0.198	0.103	0.001
HC6	0.253	0.173	0.057
HC7	−0.012	0.086	0.094
HC7	−0.019	0.169	0.056
HC8	−0.140	0.106	0.216
HC8	−0.179	0.191	0.192
HC9	−0.219	0.181	0.336
HC9	−0.065	0.226	0.330
HC10	−0.061	0.069	0.360
HC10	−0.066	0.126	0.439
HCN2	0.297	0.206	0.430
HCN2	0.147	0.244	0.390
HCN2	0.156	0.205	0.483
HCN3	0.500	0.040	0.380
HCN3	0.529	−0.047	0.347
HCN3	0.546	0.021	0.281
HCN4	0.480	0.060	0.040
HCN4	0.486	0.136	0.097
HCN4	0.529	0.058	0.141
HCN5	0.100	0.260	0.240
HCN5	0.177	0.263	0.149
HCN5	0.002	0.281	0.156

[a] Temperature factors fixed with $B = 5.0$ Å^2.

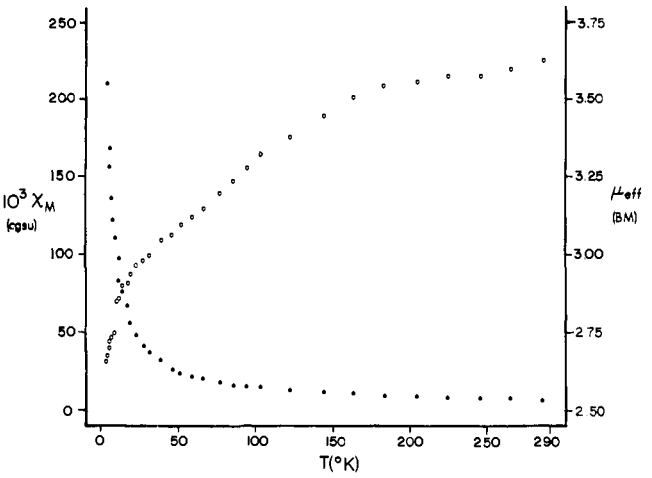

Figure 1. Temperature dependence of $\chi_{m(cor)}$ (●) and μ_{eff} (○) for $[Fe(TMC)(NO)](BF_4)_2$, isomer A.

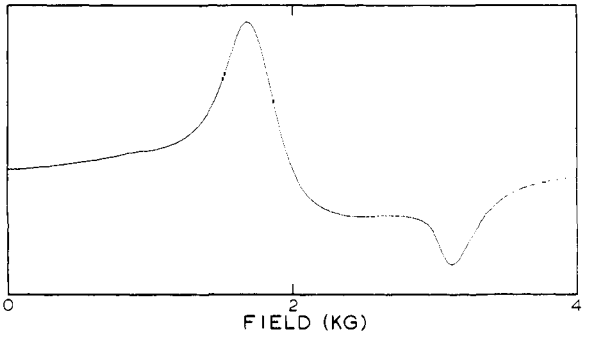

Figure 2. ESR spectrum of $[Fe(TMC)(NO)](BF_4)_2$ at ca. 8 K.

(CH_3NO_2, CH_3CN). The reaction with $NO_{(g)}$ can also be conducted in CH_3CN, where dark green solutions of the nitrosyl readily form. However, the reaction is highly reversible (purging such solutions with N_2 will rapidly and completely eliminate the color of the nitrosyl complex) and the greater insolubility of the acetonitrile complex makes it impossible to crystallize the nitrosyl complex from acetonitrile. The nitrosyl complex is much more stable in nitromethane, where NO is not rapidly lost even with a N_2 purge. The solid can be heated for several hours at 80 °C without detectable loss of NO. X-ray structure analysis, vide infra, shows that this complex is five-coordinate with a Fe-N-O bond angle of 177°.

Quantitative conversion of $[Fe(TMC)NCCH_3](BF_4)_2$ to nitrosyl products was also achieved by treating finely divided solid with $NO_{(g)}$ at about 50 psig and ambient temperature. Samples prepared in this way invariably exhibited NO stretching absorptions at 1840 and 1890 cm^{-1} but the ratio of the two absorptions varied considerably with the preparation. Samples prepared by this method will be identified as isomer AB. In all cases the lower energy band was more intense (1.5–9 times) than the higher energy band. In solution, isomer AB exhibits only the 1840-cm^{-1} absorption regardless of the composition of the solid and only the material with the 1840-cm^{-1} absorption could be reisolated in any case. We conclude that isomer AB contains isomer A and a smaller amount of a second species B with an 1890-cm^{-1} NO stretching absorption.

Isomer A shows temperature-dependent magnetic behavior with μ_{eff} ranging from about 3.62 μ_B at 286 K to about 2.66 μ_B at 4.2 K. Plots of the magnetic susceptibility and magnetic moment as a function of temperature are given in Figure 1.[13] Isomer AB also shows a similar temperature-dependent magnetic behavior.

Table III. Selected Interatomic Distances (Å), Angles (deg), and Least-Squares Planes in the Cation $[Fe(C_{14}H_{32}N_4)NO]^{2+}$

		Distances	
Fe-N(1)	1.737 (6)	N(2)-C(1)	1.477 (8)
N(1)-O	1.137 (6)	C(1)-C(2)	1.403 (10)
		C(2)-N(3)	1.513 (9)
Fe-N(2)	2.183 (5)	N(3)-C(3)	1.500 (8)
Fe-N(3)	2.147 (4)	C(3)-C(4)	1.491 (9)
Fe-N(4)	2.168 (5)	C(4)-C(5)	1.509 (9)
Fe-N(5)	2.162 (4)	C(5)-N(4)	1.488 (8)
		N(4)-C(6)	1.495 (8)
N(2)-CN(2)	1.497 (8)	C(6)-C(7)	1.477 (10)
N(3)-CN(3)	1.483 (8)	C(7)-N(5)	1.489 (7)
N(4)-CN(4)	1.492 (8)	N(5)-C(8)	1.510 (8)
N(5)-CN(5)	1.493 (7)	C(8)-C(9)	1.508 (9)
		C(9)-C(10)	1.504 (9)
		C(10)-N(2)	1.487 (8)
		Angles	
Fe-N(1)-O	177.5 (5)	N(2)-C(1)-C(2)	113.5 (6)
		C(1)-C(2)-N(3)	114.1 (6)
N(1)-Fe-N(2)	96.6 (2)	C(2)-N(3)-C(3)	107.3 (6)
N(1)-Fe-N(3)	108.0 (2)	N(3)-C(3)-C(4)	116.4 (5)
N(1)-Fe-N(4)	97.2 (2)	C(3)-C(4)-C(5)	114.7 (5)
N(1)-Fe-N(5)	105.9 (2)	C(4)-C(5)-N(4)	115.2 (5)
		C(5)-N(4)-C(6)	111.4 (5)
N(2)-Fe-N(3)	83.5 (2)	N(4)-C(6)-C(7)	111.1 (5)
N(3)-Fe-N(4)	92.6 (2)	C(6)-C(7)-N(5)	109.7 (5)
N(4)-Fe-N(5)	83.2 (2)	C(7)-N(5)-C(8)	107.7 (4)
N(5)-Fe-N(2)	92.6 (2)	N(5)-C(8)-C(9)	115.3 (5)
		C(8)-C(9)-C(10)	114.5 (5)
N(2)-Fe-N(4)	166.2 (2)	C(9)-C(10)-N(2)	114.3 (5)
N(3)-Fe-N(5)	146.1 (2)	C(10)-N(2)-C(1)	110.6 (5)
Fe-N(2)-CN(2)	112.7 (4)		
Fe-N(3)-CN(3)	112.0 (4)		
Fe-N(4)-CN(4)	114.4 (4)		
Fe-N(5)-CN(5)	109.4 (3)		

Least-Squares Planes

(a) $0.593X - 0.706Y + 0.388Z = 1.311$

atom	dev, Å
O	−0.007
N(1)	0.011
N(2)	−0.004
N(4)	−0.004
Fe	0.004

(b) $-0.384X + 0.280Y + 0.880Z = 3.134$

atom	dev, Å
O	−0.013
N(1)	0.018
N(3)	−0.004
N(5)	−0.004
Fe	0.001

(c) $0.741X + 0.658Y + 0.136Z = 2.758$

atom	dev, Å
N(2)	0.206
N(3)	−0.181
N(4)	0.135
N(5)	−0.210
Fe[a]	0.432

[a] The iron atom is not included in the determination of the plane.

EPR spectra obtained for a sample of isomer A and for a sample of isomer AB (10% isomer B) at 300 and 90 K consisted of a very broad signal with $g \approx 2$. However, at ca. 8 K the spectra consisted of prominent features at $g = 2.09$ and 3.87; see Figure 2.

Infrared spectra were measured as a function of temperature on samples of isomer AB as KBr pellets. At ca. 100 K, broadening of the 1840-cm^{-1} band was detectable, apparently the

Table IV. Final Positional and Anisotropic Thermal Parameters[a] (with esd's) for $[Fe(TMC)(NO)(OH)](ClO_4)_2 \cdot CH_3CN$[b]

atom	X	Y	Z	β_{11}	β_{22}	β_{33}	β_{12}	β_{13}	β_{23}
Fe	0.1322 (1)	−0.1740 (1)	0.0253 (1)	0.0076 (1)	0.0077 (1)	0.0088 (2)	0.0053 (1)	0.0053 (1)	0.0068 (1)
C11	−0.4024 (2)	0.4377 (2)	0.2950 (2)	0.0113 (3)	0.0129 (3)	0.0157 (4)	0.0068 (3)	0.0077 (3)	0.0108 (3)
C12	0.1687 (3)	−0.1518 (3)	0.5003 (3)	0.0245 (5)	0.0223 (5)	0.0224 (5)	0.0154 (4)	0.0172 (4)	0.0184 (4)
O1	0.2731 (7)	−0.3329 (7)	−0.0175 (7)	0.024 (1)	0.023 (1)	0.027 (1)	0.019 (1)	0.018 (1)	0.021 (1)
O2	0.0405 (4)	−0.0715 (4)	0.0497 (4)	0.0073 (6)	0.0074 (6)	0.0083 (6)	0.0063 (5)	0.0055 (5)	0.0069 (8)
P01	−0.3417 (6)	0.3624 (6)	0.3085 (7)	0.0173 (9)	0.019 (1)	0.026 (1)	0.0118 (8)	0.0126 (9)	0.019 (1)
P02	−0.468 (1)	0.486 (2)	0.372 (2)	0.071 (3)	0.083 (4)	0.077 (4)	0.070 (4)	0.068 (3)	0.073 (4)
P03	−0.5112 (9)	0.3364 (8)	0.1344 (8)	0.029 (2)	0.025 (1)	0.018 (1)	0.011 (1)	0.002 (1)	0.014 (1)
P04	−0.2795 (9)	0.5699 (9)	0.376 (1)	021 (1)	0.023 (1)	0.042 (2)	0.002 (1)	0.005 (1)	0.026 (2)
N1	0.2161 (6)	−0.2663 (7)	−0.0001 (7)	0123 (9)	0.0125 (9)	0.015 (1)	0.0091 (8)	0.0094 (8)	0.0119 (9)
N2	−0.0132 (6)	−0.3223 (6)	−0.2188 (6)	0.0085 (8)	0.0104 (8)	0.0111 (9)	0.0054 (7)	0.0059 (7)	0.0089 (8)
N3	−0.0586 (6)	−0.3203 (6)	−0.0378 (7)	0.0114 (9)	0.0125 (9)	0.014 (1)	0.0082 (8)	0.0091 (8)	0.0115 (9)
N4	0.2584 (6)	−0.0094 (7)	0.2768 (6)	0.0108 (9)	0.013 (1)	0.0095 (9)	0.0071 (8)	0.0059 (8)	0.0084 (9)
N5	0.3103 (6)	−0.0059 (6)	0.1004 (6)	0.0100 (9)	0.0082 (8)	0.0106 (9)	0.0046 (7)	0.0062 (8)	0.0065 (8)
N6	−0.554 (1)	−0.346 (1)	0.210 (1)	0.024 (2)	0.031 (2)	0.026 (2)	0.013 (2)	0.016 (2)	0.022 (2)
CN2	0.0065 (9)	−0.4546 (8)	−0.3259 (9)	0.015 (1)	0.012 (1)	0.013 (1)	0.008 (1)	0.009 (1)	0.009 (1)
CN3	−0.0364 (9)	−0.4062 (9)	−0.017 (1)	0.016 (1)	0.013 (1)	0.022 (2)	0.008 (1)	0.011 (1)	0.015 (1)
CN4	0.327 (1)	−0.055 (1)	0.336 (1)	0.018 (1)	0.023 (2)	0.017 (2)	0.014 (1)	0.011 (1)	0.018 (1)
CN5	0.4422 (8)	−0.030 (1)	0.104 (1)	0.011 (1)	0.018 (1)	0.019 (2)	0.007 (1)	0.010 (1)	0.015 (1)
C1	−0.1747 (7)	−0.3869 (8)	−0.2675 (8)	0.007 (1)	0.013 (1)	0.010 (1)	0.0035 (9)	0.0032 (9)	0.009 (1)
C2	−0.1879 (8)	−0.4454 (8)	−0.2160 (9)	0.010 (1)	0.014 (1)	0.017 (1)	0.004 (1)	0.007 (1)	0.012 (1)
C3	−0.1142 (9)	−0.2253 (9)	0.060 (1)	0.015 (1)	0.017 (1)	0.021 (2)	0.011 (1)	0.014 (1)	0.017 (1)
C4	0.008 (1)	−0.094 (1)	0.243 (1)	0.024 (2)	0.021 (2)	0.023 (2)	0.017 (2)	0.020 (2)	0.019 (2)
C5	0.155 (1)	0.0369 (9)	0.3259 (9)	0.020 (1)	0.014 (1)	0.012 (1)	0.012 (1)	0.012 (1)	0.010 (1)
C6	0.3979 (9)	0.1293 (9)	0.3654 (9)	0.011 (1)	0.013 (1)	0.011 (1)	0.004 (1)	0.005 (1)	0.007 (1)
C7	0.3684 (9)	0.1429 (8)	0.2690 (8)	0.014 (1)	0.009 (1)	0.011 (1)	0.003 (1)	0.006 (1)	0.006 (1)
C8	0.2572 (8)	0.0062 (9)	0.0032 (9)	0.013 (1)	0.013 (1)	0.015 (1)	0.006 (1)	0.009 (1)	0.012 (1)
C9	0.1629 (9)	−0.1443 (9)	−0.1790 (9)	0.018 (1)	0.017 (1)	0.018 (1)	0.010 (1)	0.012 (1)	0.016 (1)
C10	−0.0010 (9)	−0.2449 (8)	−0.2519 (8)	0.013 (1)	0.014 (1)	0.012 (1)	0.006 (1)	0.006 (1)	0.012 (1)
C11	−0.303 (1)	−0.313 (1)	0.227 (1)	0.023 (2)	0.027 (2)	0.025 (2)	0.012 (2)	0.017 (2)	0.018 (2)
C12	−0.446 (1)	−0.331 (1)	0.215 (1)	0.021 (2)	0.017 (2)	0.015 (2)	0.008 (2)	0.011 (2)	0.011 (1)

[a] The form of the expression defining the thermal ellipsoids is the same as that for footnote *a* to Table I. [b] The oxygen atoms of perchlorate ion 2 were refined isotropically; final positional parameters are given in Table V.

Scheme I

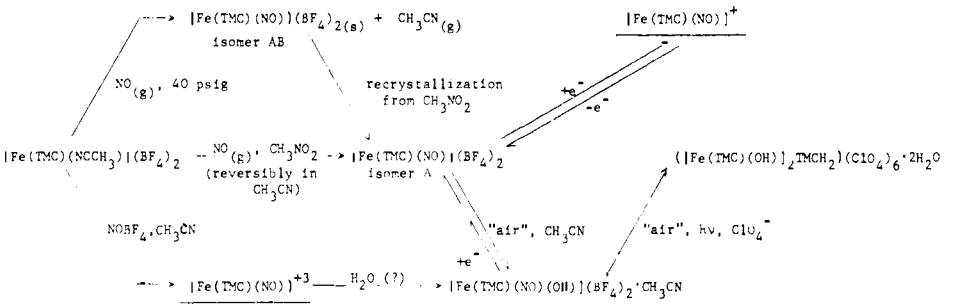

result of a band growing in at lower energy. Some additional broadening occurred as the temperature was reduced to ca. 35 K, the lower limit we could attain, but resolution of the new band was not achieved. There was no change in the 1890-cm^{-1} band over the accessible temperature range.

Iron-57 Mössbauer spectra were obtained for samples of isomer A maintained at either 300, 90, or 10 K. Figure 3 shows that at each temperature the spectrum consists of a single quadrupole-split doublet. The three spectra were least squares fit to Lorentzian lines with the two components of each doublet constrained to have equal areas. As shown in Figure 3, the signal in the 300 K spectrum has relatively poor signal to noise characteristics; however, there is clearly one asymmetric doublet with an isomer shift (δ) of +0.46 (2) mm/s vs. iron and a quadrupole splitting (ΔE_Q) of 0.53 (2) mm/s. Table VII summarizes the δ and ΔE_Q parameters obtained by fitting the three spectra; line widths are also given. An examination of the data in Table VII shows that δ changes appreciably in going from 300 to 90 K and finally to 10 K. It is relatively clear from Figure 3 that ΔE_Q is also quite temperature dependent, with the value decreasing from 300 to 90 K, then increasing from 90 to 4.2 K.

In nitromethane solution $[Fe(TMC)NO)](BF_4)_2$ is reduced at a potential of −0.87 V vs. Ag/Ag^+ (0.1 M in CH_3NO_2). The separation between the anodic and cathodic peaks in the cyclic voltammetry scan is approximately 80 mV, indicating that the process is quasi-reversible. It was not possible to observe an oxidation wave for this complex under these conditions.

$[Fe(TMC)(NO)(OH)]Y_2CH_3CN$ ($Y = BF_4^-$, ClO_4^-). This six-coordinate complex ($Y = BF_4^-$) is isolated as the main product from two different reactions, both utilizing $[Fe(TMC)NCCH_3](BF_4)_2$ as starting material. When an acetonitrile solution of the TMC complex was treated with $NOBF_4$ a dark green solution rapidly formed, which invariably turned red, although the rate varied tremendously with the individual preparation. A dark red, diamagnetic product exhibiting a nitrosyl stretching absorption at 1890 cm^{-1} was isolated from these reaction mixtures and was ultimately shown to be the above six-coordinate complex. When initially ob-

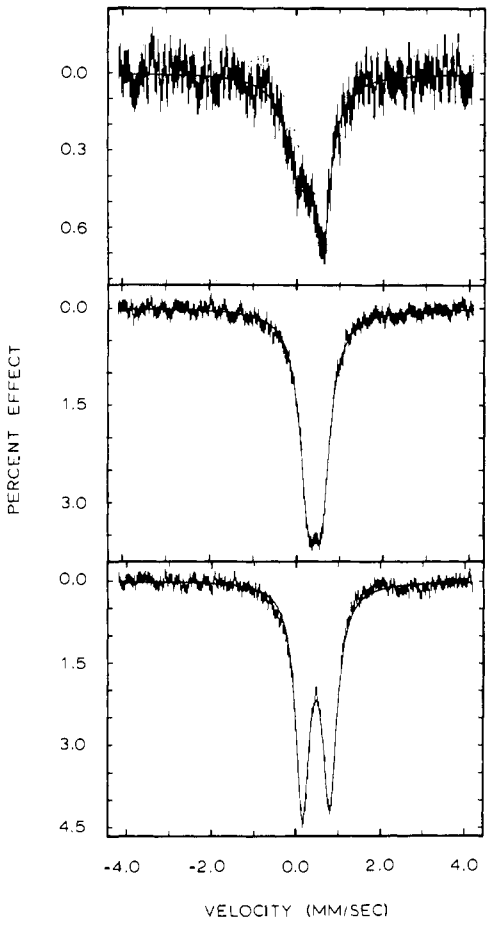

Figure 3. ^{57}Fe Mössbauer spectra of $[Fe(TMC)NO](BF_4)_2$ at 300, 90, and 10 K (top to bottom).

tained, the product was believed to be $[Fe(TMC)(NO)(NCCH_3)](BF_4)_2$ based on its apparent empirical formula (by elemental analysis), although the color change leading to its formation as well as the change in oxidation state and diamagnetism was puzzling. Subsequent preparations gave virtually identical analyses which were consistently slightly lower than theoretical. Closer inspection of data for products from several different preparations suggested that the correct formula weight was 18–20 mass units higher. Only F or O seemed to be possibilities, based on the history of the sample, and if these species were present in ionic form they must be coordinated, since concentration-dependent conductivity measurements were only consistent with a 2:1 electrolyte. In order to obtain an oxygen analysis the BF_4^- salt was metathesized to the ClO_4^- form. The result obtained is most consistent with the presence of ten oxygen atoms per formula weight (rather than the nine required if fluoride is the anion). The X-ray structure confirms the presence of the sixth ligand (but not its identity!) and shows that the acetonitrile molecule is not coordinated. In fact, the same reaction can be conducted in CH_3NO_2, where the same sequence of color changes occurs and the same complex is isolated with a molecule of CH_3NO_2 rather than CH_3CN in the lattice.

$[Fe(TMC)(NO)(OH)]^{2+}$ undergoes a nearly reversible reduction at −0.38 V (at Pt electrode vs. 0.1 M Ag^+/Ag in CH_3NO_2.) The separation between anodic and cathodic peak potentials in the cyclic voltammogram is 79 mV. A second, irreversible reduction occurs at −0.90 V. This value is very close to the potential observed for the reduction of $[Fe(TMC)NO](BF_4)_2$ in the same medium. An appealing explanation for the second reduction wave is that the reduced

Table V. Final Positional and Isotropic Thermal Parameters (with esd's) for Hydrogen Atoms and Oxygen Atoms of Perchlorate 2 of $[Fe(TMC)(NO)(OH)](ClO_4)_2 \cdot CH_3CN$

atom	X	Y	Z	B
P05	0.030 (2)	−0.294 (2)	0.324 (2)	7.0 (3)
P06	0.240 (2)	−0.214 (1)	0.534 (2)	6.2 (3)
P07	0.318 (2)	−0.010 (2)	0.608 (2)	8.3 (4)
P08	0.116 (2)	−0.063 (2)	0.516 (2)	7.9 (3)
P09	0.187 (2)	−0.163 (2)	0.585 (2)	9.2 (4)
P010	0.112 (3)	−0.273 (2)	0.335 (2)	9.0 (4)
P011	0.073 (3)	−0.163 (2)	0.545 (3)	11.1 (5)
P012	0.273 (4)	−0.165 (4)	0.460 (4)	15.8 (8)
HCN2	−0.080 0	−0.520 0	−0.440 0	5.0
HCN2	−0.005 8	−0.512 7	−0.315 8	5.0
HCN2	0.108 8	−0.416 5	−0.300 6	5.0
HCN3	0.040 0	−0.340 0	0.080 0	5.0
HCN3	−0.016 2	−0.479 7	−0.087 6	5.0
HCN3	−0.129 1	−0.462 1	−0.039 3	5.0
HCN4	0.360 0	−0.120 0	0.280 0	5.0
HCN4	0.248 7	−0.111 2	0.324 7	5.0
HCN4	0.415 0	0.035 4	0.448 4	5.0
HCN5	0.400 0	−0.120 0	0.000 0	5.0
HCN5	0.481 3	−0.037 6	0.165 5	5.0
HCN5	0.526 0	0.051 1	0.145 2	5.0
HC1	−0.248 9	−0.468 7	−0.382 9	5.0
HC1	−0.194 9	−0.306 5	−0.215 0	5.0
HC2	−0.182 4	−0.535 7	−0.279 2	5.0
HC2	−0.289 3	−0.478 7	−0.238 0	5.0
HC3	−0.206 6	−0.296 9	0.025 4	5.0
HC3	−0.147 8	−0.185 5	0.033 3	5.0
HC4	0.040 3	−0.137 3	0.265 8	5.0
HC4	−0.040 8	−0.048 8	0.293 6	5.0
HC5	0.214 9	0.117 4	0.442 5	5.0
HC5	0.125 5	0.080 9	0.302 2	5.0
HC6	0.486 3	0.122 2	0.387 5	5.0
HC6	0.421 6	0.221 9	0.469 0	5.0
HC7	0.464 1	0.225 6	0.321 5	5.0
HC7	0.292 0	0.168 9	0.263 5	5.0
HC8	0.347 3	0.079 8	0.040 3	5.0
HC8	0.192 5	0.047 3	0.022 7	5.0
HC9	0.212 2	−0.200 5	−0.200 1	5.0
HC9	0.159 8	−0.124 4	−0.229 7	5.0
HC10	−0.065 7	−0.323 6	−0.367 7	5.0
HC10	−0.040 6	−0.179 6	−0.208 7	5.0

form of $[Fe(TMC)(NO)(OH)]^{2+}$, presumably $[Fe(TMC)(NO)(OH)]^+$, loses coordinated hydroxide to generate $[Fe(TMC)NO]^{2+}$, which then undergoes reduction to $[Fe(TMC)NO]^+$. The irreversible nature of the reduction wave is not readily accounted for, although it must be kept in mind that the conditions of this experiment are necessarily different from those in which $[Fe(TMC)NO]^{2+}$ is the predominant electroactive species in solution. No oxidation of $[Fe(TMC)(NO)(OH)]^{2+}$ was observed.

The deep green precursor to the red, six-coordinate species has remained elusive. Extreme precautions were taken to exclude water from glassware, solvent, reagents, etc., but some of the red complex still formed, although usually at a reduced rate and in lower yield. Despite repeated attempts our only evidence for the existence of a five-coordinate $\{FeNO\}^6$ species is from the result of an experiment in which $[Fe(TMC)NCCH_3](BF_4)_2$ was treated with $NOBF_4$ in CH_2Cl_2. After a 24-h reaction period a green solid was obtained whose analytical data were consistent with the formulation $[Fe(TCM)NO](BF_4)_3$. Our inability to successfully repeat this experiment casts serious doubt on the existence of this complex as an isolable species.

An alternative route to $[Fe(TMC)(NO)(OH)](BF_4)_2 \cdot CH_3CN$ is the reaction of $[Fe(TMC)NCCH_3](BF_4)_2$ with $NO_{(g)}$ in CH_3CN followed by exposure of the resulting green

Table VI. Selected Interatomic Distances (Å), Angles (deg), and Least-Squares Planes in the Cation $[Fe(C_{14}H_{32}N_4)(NO)(OH)]^{2+}$ [a]

		Distances	
Fe-N(1)	1.621 (6)	N(2)-C(1)	1.487 (9)
Fe-O(2)	1.798 (3)	C(1)-C(2)	1.489 (10)
		C(2)-N(3)	1.497 (10)
N(1)-O(1)	1.143 (6)	N(3)-C(3)	1.527 (9)
		C(3)-C(4)	1.509 (13)
Fe-N(2)	2.078 (7)	C(4)-C(5)	1.499 (12)
Fe-N(3)	2.086 (7)	C(5)-N(4)	1.507 (10)
Fe-N(4)	2.107 (8)	N(4)-C(6)	1.487 (11)
Fe-N(5)	2.086 (7)	C(6)-N(5)	1.486 (10)
		C(7)-N(5)	1.489 (10)
N(2)-CN(2)	1.511 (9)	N(5)-C(8)	1.482 (9)
N(3)-CN(3)	1.509 (9)	C(8)-C(9)	1.509 (11)
N(4)-CN(4)	1.507 (9)	C(9)-C(10)	1.498 (11)
N(5)-CN(5)	1.508 (9)	C(10)-N(2)	1.502 (8)
		Angles	
Fe-N(1)-O(1)	178.3 (6)	N(2)-C(1)-C(2)	109.5 (6)
N(1)-Fe-O(2)	178.1 (3)	C(1)-C(2)-N(3)	110.2 (6)
		C(2)-N(3)-C(3)	109.3 (6)
N(1)-Fe-N(2)	95.1 (3)	N(3)-C(3)-C(4)	114.0 (6)
N(1)-Fe-N(3)	93.4 (3)	C(3)-C(4)-C(5)	118.0 (6)
N(1)-Fe-N(4)	93.5 (3)	C(4)-C(5)-N(4)	114.6 (6)
N(1)-Fe-N(5)	95.0 (3)	C(5)-N(4)-C(6)	109.2 (6)
		N(4)-C(6)-C(7)	110.9 (6)
N(2)-Fe-N(3)	84.6 (3)	C(6)-C(7)-N(5)	110.9 (6)
N(3)-Fe-N(4)	93.2 (3)	C(7)-N(5)-C(8)	108.0 (6)
N(4)-Fe-N(5)	84.5 (3)	N(5)-C(8)-C(9)	115.7 (6)
N(5)-Fe-N(2)	96.4 (3)	C(8)-C(9)-C(10)	110.6 (6)
		C(9)-C(10)-N(2)	114.5 (6)
N(2)-Fe-N(4)	171.2 (3)	C(10)-N(2)-C(1)	106.5 (6)
N(3)-Fe-N(5)	171.4 (3)		
Fe-N(2)-CN(2)	114.4 (4)		
Fe-N(3)-CN(3)	118.4 (4)		
Fe-N(4)-CN(4)	117.0 (5)		
Fe-N(5)-CN(5)	112.2 (4)		

Least-Squares Plane

$0.764X - 0.630Y + 0.136Z = 2.846$

atom	dev, Å
N(2)	−0.002
N(3)	0.002
N(4)	−0.002
N(5)	0.001
Fe[b]	0.156

[a] Distances in the acetonitrile of crystallization are C-C, 1.46 (2); C-N, 1.13 (1) Å. [b] The iron atom is not included in the determination of the least-squares plane.

solution (of $[Fe(TMC)NO]^{2+}$) to air. After a short time the solution becomes red and the red hydroxy-nitrosyl complex can be isolated. The complex is apparently formed by one-electron oxidation by O_2 or NO_2 (resulting from $NO + O_2$) and reaction with water.

$[Fe(TMC)(NO)(OH)]Y_2 \cdot CH_3CN$ is stable in the solid state but does decompose in acetonitrile solution. In early preparations of the red nitrosyl, yellow filtrates were consistently observed but well-defined products could not be obtained. Subsequently, we found that a bright yellow complex and an acid salt of TMC could be consistently obtained (after suitable workup as described in the Experimental Section) when acetonitrile solutions of the red nitrosyl were allowed to stand in the light for several days. In the dark, only the acid salt of TMC was obtained as the red color of the solution lightened but did not change to yellow. These observations suggest that a thermal decomposition pathway operates parallel to a photochemical one.

$\{[Fe(TMC)(OH)]_2 \cdot TMCH_2\}(ClO_4)_6 \cdot 2H_2O$. The structure of the yellow compound obtained from decomposition of $[Fe(TMC)(NO)(OH)]^{2+}$ is believed to be the dinuclear complex shown below based on a variety of data. These include

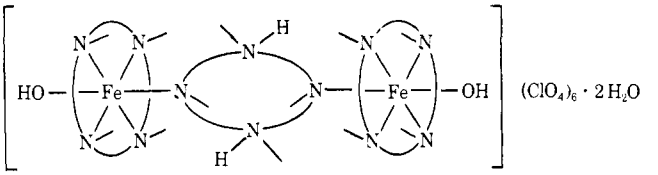

(1) consistent elemental ratios from chemical analysis (Inclusion of two water molecules gives the best agreement with the experimentally determined percentages.); (2) appearance of absorptions in the infrared spectrum expected for OH and protonated tertiary amine (3300–3100 and 2850–2650 cm^{-1}, respectively) (These absorptions diminish in intensity and new absorptions appear at lower energy for a sample recrystallized from D_2O.); (3) equivalent weight of 760 determined by pH titration (calcd 768); (4) $\mu_{eff}/Fe = 5.9\ \mu_B$ at 300 K calculated on the basis of the above formula and consistent with the +3 oxidation state for each iron (This moment was invariant with temperature to 4.2 K.); (5) $\Lambda_M = 410\ \Omega^{-1}\ cm^2\ mol^{-1}$ for a 6.9×10^{-4} M nitromethane solution.

Description of the Structure of $[Fe(TMC)NO](BF_4)_2$, Isomer A. The crystal structure of this complex consists of monomeric cations and noninteracting anions. The iron atom is five-coordinate. A perspective drawing of the cation is shown in Figure 4. A listing of selected bond angles and distances in the $[Fe(TMC)(NO)]^{2+}$ moiety is given in Table III.

The four *N*-methyl groups of the macrocyclic ligand are located on the same side of the cation giving the trans I set of nitrogen configurations according to the designation of Bosnich. The nitrosyl ligand is bonded to iron on the same side of the cation. This is the same gross structure previously determined[2] for $[Ni(TMC)N_3]^+$ and found for $[Fe(TMC)(NO)(OH)]^{2+}$ (vide infra).

A significant feature of the structure of the Fe-macrocycle moiety is the large distortion of the four nitrogen donors from planarity. In both $[Ni(TMC)N_3]^+$ and $[Fe(TMC)(NO)(OH)]^{2+}$ the four tertiary amine nitrogen donors form an exact plane and the metal atom sits above the plane on the same side as the *N*-methyl groups. In the present case N(3) and N(5) are bent considerably further away from the nitrosyl ligand than are N(2) and N(4) so that the N(3)-Fe-N(5) angle is only 146.1° whereas the N(2)-Fe-N(4) angle is 166.2°. This distortion results in a geometry intermediate between TP and TBP and represents a significant distortion compared to most of the other $\{FeNO\}^7$ systems that have been structurally characterized. It should be noted that the Fe-N distances are nominally the same, ranging from 2.15 to 2.18 Å. The distortion

Table VII. Iron-57 Mössbauer Parameters[a]

compd	*T*, K	ΔE_Q, mm/s	δ,[b] mm/s	Γ[c] mm/s
$[Fe(TMC)NO](BF_4)_2$	300	0.53 (2)	+0.46 (2)	0.36 (3), 0.23 (2)
	90	0.306 (6)	+0.538 (6)	0.241 (6), 0.233 (6)
	10	0.645 (3)	+0.588 (3)	0.195 (2), 0.204 (2)

[a] The estimated standard errors for the last significant figures are given in parentheses. [b] Relative to iron metal; to convert to $Na_2Fe(CN)_5NO \cdot 2H_2O$ standard, add 0.257 mm/s. [c] Half-width at half-maximum listed in order of increasing velocity of the peak.

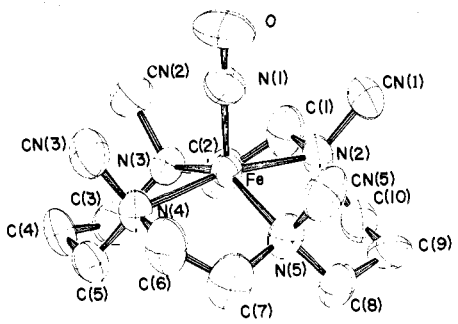

Figure 4. ORTEP drawing of the cation $[Fe(TMC)(NO)]^{2+}$. Hydrogen atoms are not shown. Thermal ellipsoids are at the 50% probability level.

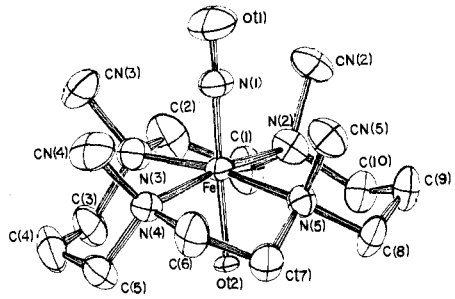

Figure 5. ORTEP drawing of the cation $[Fe(TMC)(NO)(OH)]^{2+}$. Hydrogen atoms are not shown. Thermal ellipsoids are at the 50% probability level.

from the more symmetrical TP structure results in skewing of the six-membered chelate rings away from the lower energy symmetrical chair form generally observed in complexes of 14-membered macrocyclic ligands of the cyclam class.

The nitrosyl–iron attachment is essentially linear with a Fe–N–O angle of 177.5 (5)°. The Fe–NO distance of 1.737 (6) Å is one of the longest observed for an $\{FeNO\}^7$ complex (vide infra).

Description of the Structure of $[Fe(TMC)(NO)(OH)](ClO_4)_2 \cdot CH_3CN$. The crystal structure consists of monomeric cations, noninteracting anions, and an acetonitrile molecule of crystallization. The iron is six-coordinate, being bonded to the four tertiary amine donors of the macrocyclic ligand, the nitrosyl ligand, and an hydroxide ion. A perspective drawing of the cation is shown in Figure 5. A listing of selected bond distances and angles is given in Table VI.

Distances and angles within the macrocyclic ligand are substantially the same as in $[Fe(TMC)NO]^{2+}$ and $[Ni(TMC)N_3]^+$. The Fe–N distances in the iron-macrocycle moiety are nearly the same (ranging from 2.08 to 2.10 Å) and are on the average 0.07 Å shorter than those in $[Fe(TMC)NO]^{2+}$. As observed earlier the four methyl groups occupy positions on the same side of the plane formed by the four nitrogen donors (although not crystallographically required, the four nitrogen atoms form an exact plane; see Table VI). The iron atom sits 0.156 Å out of the N_4 plane *toward* the nitrosyl ligand.

The nitrosyl group is linearly coordinated on the side of the cation bearing the methyl groups with an Fe–NO distance of 1.621 Å, which is substantially shorter than in the $\{FeNO\}^7$ system described earlier. This shortening can be ascribed to the increase in oxidation state of the metal and its diamagnetism. The Fe–N–O angle is 178.3°. The Fe–OH distance is 1.798 Å, which is in the expected range for Fe–OH bonds. The hydrogen atom was not revealed by the final difference Fourier and the identity of this ligand rests on the chemical and analytical results described in a previous section.

Inspection of Figure 5 shows that the five-membered chelate rings are staggered (as they are in the $[Ni(TMC)N_3]^+$ cation), although the 1,4-nitrogen configurations are such that eclipsed ethylene linkages might have resulted. Since a staggered ethylene linkage is lower in energy than an eclipsed, this is not surprising; however, there is considerable distortion of other parts of the tetramine molecule in order to achieve the staggered ethylene moieties. This is most readily detected in the Fe–methyl carbon distances (nonbonding). The iron to CN(3) and CN(4) distances are 3.1 Å whereas the corresponding CN(2) and CN(5) distances are only 3.0 Å. The closer proximity of CN(2) and CN(5) to the metal is dictated by the orientation of C(1) and C(7). Since these two atoms are moved down (from their expected positions in an eclipsed ring) to effect the staggering of the five-membered chelate rings, the two nitrogens to which they are attached, N(2) and N(5), are tilted more toward the metal than their counterparts N(3) and N(4), thus bringing CN(2) and CN(5) closer to the metal. Simultaneously, since the carbon atoms of the five-membered rings to which N(3) and N(4) are bound, namely, C(2) and C(6), are moved upward in the staggered conformation, N(3) and N(4) are tilted away form the metal resulting in greater distances between the metal and CN(3) and CN(4). The net result of these movements is a considerable distortion in some of the angles around the nitrogen donors and certain of the six-membered chelate ring carbons away from the expected tetrahedral angles.

Discussion

$[Fe(TMC)NO](BF_4)_2$. The relationship between molecular and electronic structure of metal nitrosyls is of considerable current interest and several bonding schemes have been presented to correlate the two, especially in the $\{MNO\}^{6,7,8}$ cases, where the structural effects of a change in the number of valence shell electrons is most evident.[15] However, all complexes to which these correlations have been applied have been of the more common low-spin variety. $[Fe(TMC)(NO)](BF_4)_2$ is one of the few $\{MNO\}^7$ systems that occurs in a high-spin form and is the first structurally characterized example.[16]

Before proceeding to a discussion of the molecular and electronic structure of $[Fe(TMC)(NO)]^{2+}$ the temperature-dependent magnetic behavior of the complex must be considered. At 270 K the effective magnetic moment of isomer A (3.6 μ_B) is consistent with a $S = 3/2$ spin state whereas the moment drops to a value of about 2.7 μ_B at 4.2 K. The latter value is somewhat greater than the spin only value for a $S = 1/2$ spin state.

Two explanations can be offered for these observations. The combined effects of the noncubic ligand field and spin–orbit coupling could give rise to splitting of the apparent quartet ground state in zero field into $M_s = \pm 3/2$ and $M_s = \pm 1/2$ levels. Changes in the magnetic moment could then be ascribed to increased population of the lower levels at the expense of the higher levels as the temperature is decreased. Inherent in this explanation is the existence of an excited state of the molecule which can interact with the quartet ground state and split the fourfold spin degeneracy. In fact, the susceptibility curves are not typical of systems in which zero-field effects are documented.[4] Zero-field interactions are normally only a few cm^{-1} in magnitude and, as a result, μ_{eff} does not decrease in value until the sample temperature is reduced below ca. 50 K. As shown by Figure 1, the decrease in μ_{eff} for $[Fe(TMC)NO](BF_4)_2$ sets in at ca. 175 K.

The alternative, preferred explanation of the magnetic behavior is the existence of a spin equilibrium between quartet and doublet states. This explanation has support from other sources. The changes in the appearance of the nitrosyl stretching absorption at low temperature are consistent with the idea that electrons are pairing up in a lower lying molecular orbital that contains a contribution from the π^* orbitals of NO

(vide infra). The appreciable temperature dependence of both δ and ΔE_Q, determined from the Mossbauer spectra, is also consistent with the idea that there is a large change in the electron distribution about the iron as might be expected for a change in spin state. Neither of these changes in observable properties is an expected consequence of a change in population of M_s states resulting from zero-field splitting. For example, the quadrupole splitting parameter of $[Fe(TMC)N_3]BF_4$, a complex which shows zero-field splitting of the $^5B_2$ ground state, hardly changes on going from 100 to 4.2 K (the values are 0.877 and 0.899 mm s^{-1}, respectively).[4]

Finally, it should be noted that the magnetic behavior and infrared spectral behavior of $[Fe(TMC)(NO)]^{2+}$ are quite similar to that observed for a series of five-coordinate mononitrosyl complexes of iron with salen (salen = *N,N'*-ethylenebissalicylideniminato) and several of its ring-substituted derivatives.[6] Most of these complexes have a magnetic moment corresponding to three unpaired electrons at room temperature. For the unsubstituted derivative, Fe(salen)NO, a sharp transition in the μ_{eff} vs. temperature curve was observed at ca. 180 K. Concomitant with the change in spin state, the nitrosyl stretching absorption of the complex shifts to lower energy in the infrared spectrum. In addition to Fe(salen)NO, five other NO complexes with a substituted salen ring were studied. In every case except one, μ_{eff} was found to be temperature dependent; however, the decrease in μ_{eff} with decreasing temperature was found to be more gradual. For example, in the case of Fe(4-Cl-salen)NO, μ_{eff} varies gradually from 4.03 μ_B at 300 K to 3.59 μ_B at 90 K. These complexes are considered to exhibit $S = 3/2$–$1/2$ spin-state equilibria; their behavior is very similar to that observed for $[Fe(TMC)NO](BF_4)_2$. It appears likely, then, that the temperature dependence of μ_{eff} observed for this TMC complex reflects a depopulation of an $S = 3/2$ excited state with concomitant increase of Boltzmann population in the $S = 1/2$ ground state.

The distortion of the structure of $[Fe(TMC)(NO)]^{2+}$ from tetragonal pyramidal (TP) toward trigonal bipyramidal (TBP), which involves a good deal of distortion of the TMC ligand, was initially quite surprising in view of the very regular structures displayed by $[Ni(TMC)N_3]^+$ and $[Fe(TMC)(NO)(OH)]^{2+}$ and the very symmetrical structures found for other {FeNO}^{7} systems. The 1840-cm^{-1} infrared stretching absorption also seemed quite high even for a {FeNO}^{7} complex.[17] However, we subsequently concluded that both of these features might be a natural consequence of the electronic structural features of this cation and that even a qualitative bonding description of the molecule must explain the $3/2$ spin state, the distorted structure, and the high NO stretching frequency.

Of the several molecular orbital schemes that have been proposed to account for the structure and bonding of five-coordinate mononitrosyls,[15] none can be used without modification to explain both the quartet state and the distortion observed for $[Fe(TMC)(NO)]^{2+}$. The most obvious difference between $[Fe(TMC)(NO)]^{2+}$ and other five-coordinate {FeNO}^{7} systems is the very weak ligand field strength and complete absence of π-bonding capability of the TMC ligand compared to basal ligands of other systems. The weak ligand field strength of the tetramine has been inferred from spectroscopic studies on Ni(II) complexes.[2,18] By incorporating this feature into the MO schemes proposed by other workers both the quartet state and the distortion of $[Fe(TMC)(NO)]^{2+}$ can be accounted for.

Figure 6 gives a qualitative energy level diagram for an idealized five-coordinate MNO molecule having C_{2v} symmetry; the dotted lines show the expected direction of changes in the energies of these levels on going from C_{4v} to C_{2v} symmetry. In C_{2v} symmetry d_{xz} and d_{yz} are split with d_{yz} raised in energy because of the increase in interaction with ligands

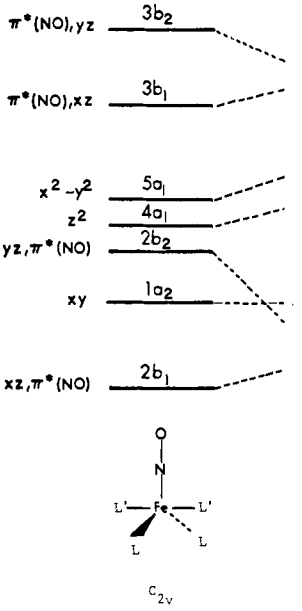

Figure 6. Qualitative energy level diagram for $[Fe(TMC)(NO)]^{2+}$ assuming C_{2v} symmetry. The Fe–NO bond is collinear with the *z* axis.

L; at the same time, $d_{x^2-y^2}$ is lowered in energy because of the reduced interaction with L. Thus the $2b_2$, 4a, and 5a levels can be near enough in energy so that when seven electrons are added, each of the levels is singly occupied at room temperature, a situation that probably could arise with the present ligand set in C_{4v} symmetry only when the L–Fe–NO angles are quite large. Single occupancy of the b_2 level, which is composed of π^*_{NO} and d_{yz}, should result in a high NO stretching frequency but double occupancy of this level, which is expected at low temperature where a significant fraction of the molecules are in the doublet state, would result in a decreased NO bond order and a decrease in the NO stretching frequency. It should be noted that pairing of the electrons in the b_2 orbital leaves d_{z^2} singly occupied, which is the ground state of other low-spin {FeNO}^{7} systems. Although all of the factors that offset what we believe to be an energetically unfavorable distortion of the Fe(TMC) moiety from the more symmetrical form that occurs in $[Ni(TMC)N_3]^{2+}$ and $[Fe(TMC)(NO)(OH)]^{2+}$ are not obvious, the favorable increase in electron correlation energy and decrease in electron–electron repulsion of the quartet state must play an important role. Whether or not there is a significant structural change with the conversion to the doublet state form at low temperature is an interesting question that has not been addressed in this study. A structure determination of $[Fe(TMC)NCCH_3](BF_4)_2$ was undertaken in order to determine that the distortion of the TMC ligand occurred during the reaction with NO. However, as outlined in the Experimental Section, the structure was disordered to the extent that it could not be solved.

The Fe–NO distance of 1.737 Å found for $[Fe(TMC)(NCl)]^{2+}$ is somewhat longer than distances in other isoelectronic five-coordinate systems (distances range from a low of 1.565 Å for $Fe(CN)_4NO^{2-}$ to a high of 1.717 Å for [Fe(TPP)NO]; see ref 15 and 19 for a tabulation of other values). This long bond distance coupled with the observation that the NO group is readily substituted by CH_3CN suggests that the NO is only weakly interacting with the metal ion.

The distortion of the Fe(TMC) moiety must be considered unusual since of the seven other structures of five-coordinate {FeNO}^{7} only one, $\{Fe[SCH_2CH_2N(CH_3)(CH_2)_2N(CH_3)CH_2CH_2S](NO)\}$,[19] shows a significant distortion from TP geometry. Lippard and co-workers concluded that the $Fe(N_2S_2)(NO)$ system was closer to TP than TBP, based, in

Table VIII. Geometrical Analysis of $[Fe(TMC)(NO)]^{2+}$ [a]

		δe_1	δe_2	δa_2	δa_5	$\delta a_{1,3,4,6}$
calcd, TP[b]		71.4	71.4	71.4	71.4	130.6
	$\Delta(\delta)$	−8.2	−9.3	+8.6	+9.2	−12.8
actual		63.2	62.1	80.0	80.6	117.8 (av)
	$\Delta(\delta)$	+15.1	+14.0	−2.8	−2.2	+21.4
calcd, TBP (C_{2v})[c]		48.1	48.1	82.8	82.8	96.4

[a] Utilizing dihedral angle method outlined by Muetterties and Guggenberger.[20] [b] For idealized FeL_4L' structure of C_{4v} symmetry with Fe-L distances of 2.16 Å, a Fe-L' distance of 1.74 Å, and a L-Fe-L' angle of 102°. [c] For idealized FeL_4L' structure of C_{2v} symmetry with Fe-L distances of 2.16 Å, a Fe-L' distance of 1.74 Å, basal angles of 120°, and basal-apical angles of 90°.

part, on the dihedral angle method of analysis suggested by Muetterties and Guggenberger.[20] Application of this method to $[Fe(TMC)NO]^{2+}$ (Table VIII) indicates that the iron atom and ligating atoms of this cation form a highly regular species that lies on a potential surface connecting TP and TBP $FeN_4(NO)$ moieties by a Berry pseudorotation but is probably closer to the TP form.

The Mössbauer data for $[Fe(TMC)NO](BF_4)_2$ require further comment. If this molecule is a $S = {}^3/_2$–$^1/_2$ spin equilibrium system, the single quadrupole-split doublet observed for the compound in the range of 10–300 K (see Figure 3) indicates that the rate of spin flipping (i.e., the rate that a given molecule interconverts between the low-spin and high-spin states) is greater than can be observed with ^{57}Fe Mössbauer spectroscopy. The spin-flipping rate is thus greater than ca. 10^7 s^{-1} and the doublet seen at each temperature has δ and ΔE_q values that are Boltzmann weighted averages reflecting the δ and ΔE_Q values for the doublet and quartet states and the relative amounts of molecules in the sample that are in either state. The same comments apply to Fe(salen)NO, which is reported[21] to show a single quadrupole-split doublet with $\Delta E_Q = 0.69$ mm/s at 193 K.

The presence of a single quadrupole-split doublet that is relatively independent of temperature for a spin-equilibrium complex is reminiscent of Mössbauer data reported[22,23] for trisdithiocarbamate ferric complexes, $Fe(S_2C\text{-}NR_2)_3$. These complexes also show only a single doublet at any temperature. The temperature dependencies of δ and ΔE_Q are also not nearly as pronounced as might be expected for an $S = {}^5/_2$–$^1/_2$ spin equilibrium. However, variable-temperature magnetic susceptibility data clearly indicate that these $Fe(S_2CNR_2)_3$ complexes are spin-equilibrium complexes.[24] Laser temperature-jump relaxation studies[25] have shown that the spin-flipping rates for the $Fe(S_2CNR_2)_3$ species are greater than ca. 10^9 s^{-1}, in agreement with the Mössbauer data.

The ca. 8 K EPR spectrum for $[Fe(TMC)NO](BF_4)_2$ with signals at $g = 2.09$ and 3.87 is also intriguing. It is only at low temperature that a resolved spectrum can be seen. Examination of the spectrum in Figure 2 shows that the low-field signal is the perpendicular signal, $g_\perp = 3.87$, and the high-field signal is the parallel signal with $g_\parallel = 2.09$. These signals must arise from the $S = {}^1/_2$ ground state. It was suggested above that this ground state corresponds to the $d_{z^2}{}^1$ electron configuration, as found in other low-spin $\{FeNO\}^7$ systems. The fact that the $g_\parallel$ signal is found to be relatively close to the free electron value is in keeping with this assignment. It is interesting that the $g_\perp$ value deviates appreciably from a $g = 2.0$ value. A relatively anisotropic g tensor was also found for the $Fe(S_2CNR_2)_3$ complexes, where, for example, for $Fe(S_2CN(CH_3)_2)_3$ a spectrum was obtained at 12 K with $g_\parallel = 3.27$ and $g_\perp$ 1.66. In the case of the ferric dithiocarbamates, it was suggested that appreciable metal-ligand covalency and spin-orbital effects led to electronic states that are very vibronic in nature.[24] In $[Fe(TMC)NO](BF_4)_2$, the bonding between the iron ion and the nitrosyl ligand is certainly quite covalent and the one-electron molecular orbitals are probably quite mixed. The quartet and doublet states could be quite vibronic and mixed to a certain degree and such mixing would account for a rapid spin-flipping rate.

Although we have no direct evidence concerning the structure of the second form of $[Fe(TMC)(NO)](BF_4)_2$ (isomer B), its existence and extremely high (1890 cm^{-1}) nitrosyl stretching frequency merit some discussion.[26] The fact that isomer B exists only in the solid state and is not detectable in solution indicates that it either decomposes to a product without a nitrosyl ligand or, perhaps more likely, that it converts readily to isomer A. The very high NO stretching frequency definitely rules out a bent Fe–NO structure and suggests a Fe^I–NO^+ formulation with very weak π bonding. If one considers possible mechanisms for the solid state conversion of $[Fe(TMC)NCCH_3](BF_4)_2$ to the mixture of nitrosyl complexes, two plausible routes are frontside displacement of NO and backside displacement followed by reaction with a second molecule of NO to give product. Some of the intermediate generated by the latter route, which would have the nitrosyl group on the side opposite the *N*-methyl groups, might be trapped in the lattice and be detected in the infrared spectrum. Obviously, a distorted form of isomer A in which the NO ligand is bonded on the same side of the complex as the methyl groups cannot be discounted.

$[Fe(TMC)(NO)(OH)]^{2+}$. The structure of the $[Fe(TMC)(NO)(OH)]^{2+}$ cation is that expected for a diamagnetic six-coordinate $\{FeNO\}^6$ compound; the linear Fe–NO grouping is predictable for six-coordinate complexes of the $\{MNO\}^6$ variety.[5] Not unexpectedly, the metal ion is located above the plane defined by the four nitrogens toward the NO ligand. This is due in part to the better ligating properties of NO as compared to OH^-, and to the steric crowding which would result if the metal were coplanar with the macrocycle. An investigation of space-filling models reveals that coplanarity of the donors and metal causes the methyl groups to occupy positions very close to the nitrosyl. Lifting the metal ion out of the plane slightly allows the nitrogens to bend back a small amount, thus relieving the steric crowding but maintaining a planar array of donors. In $[Fe(TMC)(NO)(OH)](ClO_4)_2{\cdot}CH_3CN$ the iron is 0.156 Å above the plane, whereas in $[Ni(TMC)N_3]ClO_4$ the metal is situated 0.33 Å out of the macrocyclic plane.[7] The large difference is probably due to the smaller size of the low-spin Fe(III) compared to Ni(II), as well as the six-coordinate geometry of the iron compound. Although the nature of the sixth ligand in this complex was in doubt initially, we feel that the results of the characterization are most compatible with the presence of OH^-.

Considerable effort was made to isolate $[Fe(TMC)(NO)]^{3+}$. Its lifetime was unpredictable, even when the most strenuous precautions were taken with reagents and glassware. We believe that it reacts with adventitious water to yield the more stable $[Fe(TMC)(NO(OH)]^{2+}$. The formation of the hydroxy-nitrosyl from $[Fe(TMC)(NO)]^{2+}$ probably involves oxidation by O_2 or NO_2 (from NO + $^1/_2O_2$). The fact that $[Fe(TMC)NO]^{2+}$ does not undergo electrochemical oxidation is somewhat surprising but it must be noted that the data presented were obtained on CH_3NO_2 solutions. In fact, $[Fe(TMC)(NO)]^{2+}$ appeared to undergo irreversible electrochemical oxidation in CH_3CN but the electrochemistry in this solvent is complicated by the equilibrium $[Fe(TMC)(NO)]^{2+} + CH_3CN \rightleftarrows [Fe(TMC)(NCCH_3)]^{2+} + NO$, whose products are electroactive in the same potential range as the green nitrosyl complex (+0.9 to +1.25 V). A reasonable explanation is that there is a large solvent effect on the oxidation potential that is probably connected with the considerably greater donor properties of CH_3CN compared to CH_3NO_2.

The yellow binuclear Fe(II) complex derived from decomposition of the red nitrosyl defied characterization for some time. Consequently, the actual details of the decomposition reaction were not extensively studied. Air (presumably water or O_2) is probably necessary for the dark (thermal) reaction since solutions of the complex kept in an inert atmosphere did not deposit ligand salt. Specific photochemical studies were not made. The low, single pK_a value observed for this complex is a bit surprising, but since the only "communication" between the two protonated amine nitrogens is through space, the presence of the large, charged substituents on the other two nitrogen atoms [Fe(TMC) units] may force a conformation on the bridging TMC moiety such that this interaction is too small to observe two, separate deprotonation steps.

Acknowledgments. Financial support for this research from the National Institutes of Health (D.N.H., Grant HL13652) and the National Science Foundation (E.K.B., Grants MPS 73-08709 and CHE 76-21758) is gratefully acknowledged. We also thank Dr. R. D. Feltham for his helpful comments concerning the manuscript.

Supplementary Material Available: Structure factor tables for $[Fe(TMC)NO](BF_4)_2$ and $[Fe(TMC(NO)(OH)](ClO_4)_2 \cdot CH_3CN$ and magnetic susceptibility data for one sample of $[Fe(TMC)NO](BF_4)_2$, isomer A and two samples of isomer AB (30 pages). Ordering information is given on any current masthead page.

References and Notes

(1) (a) Georgia Institute of Technology. (b) University of Illinois. (c) Camille and Henry Dreyfus Teacher-Scholar Fellow, 1972-1977; A. P. Sloan Foundation Fellow, 1976-1978.
(2) (a) E. K. Barefield and F. Wagner, *Inorg. Chem.*, **12**, 2435 (1973); (b) M. J. D'Aniello, Jr., M. T. Mocella, F. Wagner, E. K. Barefield, and I. C. Paul, *J. Am. Chem. Soc.*, **97**, 192 (1975).
(3) R. Buxtorf, W. Steinman, and T. A. Kaden, *Chimia*, **28**, 15 (1974).
(4) K. D. Hodges, R. G. Wollmann, E. K. Barefield, and D. N. Hendrickson, *Inorg. Chem.*, **16**, 2746 (1977).
(5) J. H. Enemark and R. D. Feltham, *Coord. Chem. Rev.*, **13**, 339 (1974).
(6) A. Earnshaw, E. A. King, and L. F. Larkworthy, *J. Chem. Soc. A*, 2459 (1969).
(7) E. K. Barefield, *J. Chem. Educ.*, **50**, 697 (1973).
(8) N. F. M. Henry and K. Lonsdale, Ed., "International Tables for X-ray Crystallography", Vol. I, Kynoch Press, Birmingham, England, 1965.
(9) In addition to the software package for the Syntex $P2_1$, diffractometer programs utilized include Zalkin's FORDAP Fourier summation program, Ibers' NUCLS5 modification of the Busing-Martin-Levy ORFLS full-matrix least-squares program, the Busing-Martin-Levy ORFFE function and error program, Johnson's ORTEP and ORTEPII plotting programs, and various locally written ones.
(10) D. T. Cromer and J. T. Waber, *Acta Crystallogr.*, **18**, 104 (1965).
(11) R. F. Stewart, E. R. Davidson, and W. T. Simpson, *J. Chem. Phys.*, **42**, 3175 (1965).
(12) D. T. Cromer, *Acta Crystallogr.*, **18**, 17 (1965).
(13) Susceptibility data used to construct these plots are given in the supplementary material. Also included are data sets for two other samples.
(14) B. Bosnich, C. K. Poon, and M. L. Tobe, *Inorg. Chem.*, **4**, 1102 (1965).
(15) J. H. Enemark, R. D. Feltham, B. T. Huie, P. L. Johnson, and K. B. Swedo, *J. Am. Chem. Soc.*, **99**, 3285 (1977), and references cited therein.
(16) Enemark and Feltham are conducting structural and physical methods studies of the [Fe(salen)NO] system: R. D. Feltham, private communication; K. J. Haller, Ph.D. Dissertation, University of Arizona, 1978.
(17) The NO stretching frequency of $Fe(das)_2NO$ (das = *o*-phenylenebisdimethylarsine), 1760 cm^{-1}, is the highest previously recorded for a structurally characterized $\{Fe(NO)\}^7$; see Table VIII, ref 15.
(18) D. Gatteschi and A. Scozzafava, *Inorg. Chim. Acta*, **21**, 223 (1977).
(19) K. D. Karlin, H. N. Rabinowitz, D. L. Lewis, and S. J. Lippard, *Inorg. Chem.*, **16**, 3262 (1977).
(20) E. L. Muetterties and L. J. Guggenberger, *J. Am. Chem. Soc.*, **96**, 1748 (1974).
(21) H. Mosbaek and K. G. Poulsen, *Acta Chem. Scand.*, **15**, 2421 (1971).
(22) P. B. Merrithew and P. G. Rasmussen, *Inorg. Chem.*, 11, 325 (1972), and references cited therein.
(23) R. Richards, C. E. Johnson, and H. A. O. Hill, *J. Chem. Phys.*, **53**, 3118 (1970).
(24) G. R. Hall and D. N. Hendrickson, *Inorg. Chem.*, **15**, 607 (1976).
(25) E. V. Dose, M. A. Hoselton, N. Sutin, M. F. Tweedle, and L. J. Wilson, *J. Am. Chem. Soc.*, **100**, 1141 (1978).
(26) The similarity in NO value for this species to that of $[Fe(TMC)(NO)(OH)](BF_4)_2 \cdot CH_3CN$ is coincidental. If the latter species were to exist in the solid state reaction mixture it would have to be in solvent-free form and an equal amount of a third nitrosyl complex, $[Fe(TMC)NO]BF_4$, would also have to be present to account for the analytical results.

The Chemical Evolution of a Nitrogenase Model. 17. Simulation of Steric and of Inhibitory Effects at the Enzymic Active Site with Acetylenes and Nitriles as the Substrates, and "Molybdoinsulin" Catalysts

Barbara J. Weathers, John H. Grate, and G. N. Schrauzer*

Contribution from the Department of Chemistry, University of California at San Diego, Revelle College, La Jolla, California 92093. *Received July 17, 1978*

Abstract: Stoichiometric combinations of the reduced peptide chains A and B of bovine insulin with MoO_4^{2-} reduce C_2H_2 at virtually the same rate but with lower selectivity, as the "iron-molybdenum cofactor" of nitrogenase, with $NaBH_4$ as the reducing agent. The reduction of C_2H_2 is inhibited by CO, and under certain conditions also by N_2. These "molybdoinsulin" model systems of nitrogenase simulate some of the steric hindrance effects in the reduction of substituted *acetylene* and of saturated and unsaturated *nitriles* observed under enzymatic conditions. The results of binary systems studies with a catalytic variant of the method of continuous variation are consistent with the formation of catalytically active complexes through the interaction of molybdenum with the six Cys-SH and the two His-imidazole residues of the reduced insulin peptides.

Recently, Shah and Brill[1a] reported the isolation of an "iron-molybdenum cofactor" (FeMo-co) from *Azotobacter vinelandii* nitrogenase (N_2-ase). It consists[2b] of a small peptide (or peptides) containing one Mo, eight Fe, and six labile S^{2-}. This cofactor reduces C_2H_2 to C_2H_4 at 8% of the rate of N_2-ase (on the same per-molybdenum basis), with $NaBH_4$ as the reductant.[2] The reduction of C_2H_2 was found to be inhibited by CO, but is apparently not stimulated by ATP. Nitrogen could not be reduced detectably under the conditions employed thus far.

Independently, we have been investigating new versions of N_2-ase model systems in which small peptides are the ligands of molybdenum. The initial aim of our studies was to increase the activity and selectivity of the "molybdothiol" model sys-

0002-7863/79/1501-0917$01.00/0